Applied Surface Science 720 (2026) 165249

Contents lists available at ScienceDirect

Applied Surface Science

journal homepage: www.elsevier.com/locate/apsusc

Full Length Article

Poly(dopamine)-coated TiO_2/SiO_2 resonators for the non-plasmonic SERS detection of organic analytes

Autchariya Boontanom [a], Leonardo Moscolari [b], Erika Kozma [b], Michele Speziani [c,d], Ivano Alessandri [a,d,e], Francesco Galeotti [b], Irene Vassalini [a,d,e,*]

[a] Department of Information Engineering, University of Brescia, via Branze 38, 25123 Brescia, Italy
[b] Istituto di Scienze e Tecnologie Chimiche "Giulio Natta", Consiglio Nazionale delle Ricerche, Via A. Corti 12, 20133 Milano, Italy
[c] Department of Mechanical and Industrial Engineering, University of Brescia, via Branze 38, 25123 Brescia, Italy
[d] INSTM, UdR Brescia, Italy
[e] INO-CNR, Via Branze 38, 25123 Brescia, Italy

ARTICLE INFO

Keywords:
SERS substrates
Non-plasmonic SERS
Polydopamine
Bioinspired
Histamine

ABSTRACT

Polydopamine (PDA) is a bioinspired polymer with strong adhesive properties, enabling easy surface functionalization. These abilities have already been exploited to develop advanced plasmonic and hybrid surface-enhanced Raman scattering (SERS) platforms, but the possibility of applying PDA coatings to optimize non-plasmonic SERS substrates has to be explored. Here, we applied PDA coatings to non-plasmonic SERS substrates based on core/shell SiO_2/TiO_2 micrometric spheres (T-rex), which act as dielectric resonators. Functionalized T-rex substrates were tested for the detection of methylene blue (MB), a conventional Raman probe, and histamine, a food contaminant. Compared to unmodified substrates, the PDA-coated T-rex exhibited a substantial increase in SERS activity and a reduction in detection limits (1 μM for MB and 0.01 μM for histamine). This enhancement arises from the insurrection of analyte–surface intermolecular interactions (H-bonds, π–π stacking and electrostatic attraction) and from charge-transfer processes mediated by PDA. These results demonstrate that PDA is an effective and versatile modifier to boost the sensitivity of non-plasmonic SERS substrates.

1. Introduction

In recent years, dielectric materials have gained significant attention as substrates for enhancing Raman scattering. These materials enable a wide range of optical and geometrical effects, including morphology-dependent resonances, whispering gallery modes, light trapping, and multiple scattering, which can enhance the Raman signal of analytes near their surface. [1] Unlike traditional plasmonic substrates, which rely on metal-based nanostructures, dielectric materials are characterized by low optical losses, minimizing heating effects during Raman measurements and analyte degradation. This improves both the reliability and reproducibility of Surface-Enhanced Raman Scattering (SERS) experiments. Additionally, dielectrics generally exhibit higher chemical inertia and stability, limiting the occurrence of undesired side reactions during analyte detection.

A particularly relevant example of non-plasmonic Raman enhancers is represented by T-rex, core/shell structures consisting of a low-refractive-index SiO_2 spherical core with micrometric dimensions and a high-refractive-index TiO_2 shell with nanometric thickness. The high refractive index contrast with the background (higher than 2:1) and the spherical shape facilitate multiple light scattering within the T-rex, increasing the optical path of photons and creating a light-trapping effect. This leads to a strong confinement of the electromagnetic field at their surface. The resulting evanescent field can amplify the Raman signal of analytes adsorbed at the surface of the resonator, enabling their SERS detection through the so-called electromagnetic enhancement. [2] Precedent studies conducted by our research group have demonstrated that the achieved electromagnetic field enhancement (i.e. $|E|^2/|E_{inc}|^2$ calculated through numerical simulation, where E stands for the intensity of the electromagnetic field at the T-rex surface, while E_{inc} is the intensity of the incident electromagnetic field) varies according to the thickness of the TiO_2 layer (investigated range: 10–100 nm), reaching a maximum value in the order of 10 for T-rex obtained with a TiO_2 layer of ~95 nm. [3] On the other hand, in previous studies we demonstrated

* Corresponding author at: Department of Information Engineering, University of Brescia, via Branze 38, 25123 Brescia, Italy.
E-mail address: irene.vassalini@unibs.it (I. Vassalini).

https://doi.org/10.1016/j.apsusc.2025.165249
Received 8 August 2025; Received in revised form 5 November 2025; Accepted 12 November 2025
Available online 13 November 2025

that the achieved effect is significantly different from the one obtained by employing simple SiO_2 microspheres (same diameter but lacking the TiO_2 shell layer). Pure Silica microbeads, in fact, are characterized by a refractive index contrast between the sphere and the background lower than 2:1 and they cannot concentrate the electromagnetic field around their surface, but they can behave as microlenses and give rise to the so-called "nanojet". [4] This is a narrow (lateral size ~ λ/3) non-evanescent and non-resonant beam which can originate from the shadow-side of a dielectric sphere irradiated by a light source of wavelength λ lower than the microsphere diameter, and which can be exploited to enhance the Raman signal of analytes underlying the microsphere.

Despite the great advantages of low analyte perturbation, high stability, and analysis reproducibility provided by non-plasmonic substrates, these materials typically exhibit lower enhancement factors (generally in the order of 10^2–10^3) compared to plasmonic counterparts (which can lead to enhancement factor as high as 10^8–10^{10}, leading to the possibility of single molecule detection). This limitation has hindered the widespread adoption of non-plasmonic substrates in SERS experiments, making the investigation of strategies to maximize the SERS effect in dielectric substrates an active area of research.

Different approaches have been proposed to increase their sensitivity, including engineering the properties of the dielectric material (e.g., controlling the concentration of oxygen vacancies [5]), combining dielectric materials with plasmonic components to create hybrid SERS substrates [1], or manipulating the morphology of the dielectric resonators). For example, in previous studies on core/shell resonators, we investigated the effects of varying the refractive index contrast—by using ZrO_2 [6] or Si [7] instead of TiO_2—as well as the effects of the roughness and conformality of the TiO_2 layer [8] or the addition of smaller secondary scattering centers [9] on the surface of standard T-rex.

In this work, we investigated an alternative strategy, based on pairing T-rex structures with a thin layer of polydopamine (PDA), a biodegradable and biocompatible polymer resulting from the autoxidation of dopamine in weakly alkaline solutions. Interestingly, PDA shares chemical similarities and properties with melanin, a catechol amino acid abundant in mussel adhesive proteins. In fact, one of the PDA's key properties is its high adhesion capability to a wide range of materials, a feature that has been widely exploited in the preparation of PDA-containing SERS substrates.

PDA's catechol groups have the unique ability to reduce metal ions without the need for additional reducing agents and this intrinsic property permits to induce the in-situ formation of metallic crystals, optimizing the spatial distribution of hot spots within plasmonic SERS substrates and maximizing both the efficiency and reproducibility in detecting different analytes [10–15]. The reduction properties have also been exploited to facilitate and control the formation of oxygen vacancies in MoO_3 nanosheets and increase their stability, inducing a plasmonic behavior inside the metal oxide, useful for SERS applications [16].

PDA layers have also been exploited for the fabrication of hybrid-SERS substrates to maximize the stability of the aggregation of the different subunits and facilitate charge transfer process. For example, PDA has been used to ensure a strong attachment of plasmonic NPs on dielectric surfaces, such as TiO_2 nanorod arrays [17], ZnO thin films [18], ZnO nanorods [19], MoS_2 nanosheets [20], CuO-coated glass microfiber filters [21] and even biopolymer substrates [22]. Alternatively, the remarkable adhesiveness and biocompatibility of PDA have been extensively used for the preparation of SERS tags for SERS imaging experiments [12,23,24]. Further examples of plasmonic or hybrid SERS substrates containing PDA can be found in the recent review by Tian et al.[25].

However, the adhesive properties of PDA can be exploited not only to increase the structural stability of the SERS substrates, by tightly wrapping the different building blocks inside a unique structure, but also to promote the agglomeration/concentration of an analyte in proximity to the substrate surface [26]. Surprisingly, this aspect has received little attention so far, and only few studies have explored the interactions between PDA contained in SERS substrates and target analytes.

In this work we examined, for the first time, the potential of using PDA to enhance the SERS activity of a non-plasmonic substrate. In particular, we investigated the possibility of exploiting the PDA's high density of functional groups—including amine, hydroxyl, catechol, quinone, and aromatic groups— to induce effective interactions with organic analytes. These interactions include π–π stacking, hydrogen bonding, electrostatic interactions and covalent bonds [17,27,28].

Specifically, we tested PDA-functionalized T-rex structures for the detection of a standard analyte, the organic dye methylene blue, and histamine, a potentially hazardous food contaminant. Histamine can accumulate to high concentration in canned fish or fermented beverages due to improper storage conditions. Consumption of such contaminated food and beverages can induce toxic effects similar to allergic reactions, leading to symptoms such as urticaria, eczema, diarrhea, and bronchial spasms. Traditionally, histamine detection relies on techniques such as high-performance liquid chromatography (HPLC), gas chromatography, electrochemical methods, and enzyme-linked immunosorbent assays (ELISA). However, these methods are often time-consuming and require complex sample preparation. In contrast, SERS-based detection provides a faster and more straightforward alternative.[29].

The feasibility of histamine detection through SERS has been already demonstrated [30–35], reaching detection limits below the permitted concentration threshold for food, but the use of non-plasmonic substrates in this context has yet to be explored.

Our study demonstrated that the addition of an overcoating PDA layer to T-rex substrates effectively improved their SERS activity. We investigated the underlying reasons for this improvement and examined the effect of varying the incubation time with a dopamine solution (10 min-4 h), leading to a variable thickness of the overcoating PDA layer. Our study showed that an intermediate value of incubation time (2 h) enabled to maximize the enhancement effect by limiting drawbacks, such as the interference of PDA Raman peaks during the detection of the analyte of interest or an excessive fluorescence background. Finally, we demonstrated that the PDA 2 h-Trex monolayer substrate enabled an efficient detection not only in the case of methylene blue, but also in the case of histamine. These results show that the addition of the PDA coating is an effective strategy to maximize the interaction between the SERS substrate and an organic analyte, with which PDA can create favorable bindings through H-bonds, π–π stacking and electrostatic interactions.

2. Materials and methods

2.1. Preparation of T-rex

T-rex core/shell resonators were obtained by depositing TiO_2 (nominal thickness: 100 nm) on silica microspheres (size: 2.06 ± 0.05 μm, Microparticles-GmbH) using Atomic Layer Deposition (ALD) technique, in a Savannah 100 flow reactor, according to the procedure described in our previous studies.[3,36] Briefly, ALD deposition were performed at 90 °C and 0.5 Torr using tetrakis(dimethylamino)titanium (IV) (TDMAT, Sigma-Aldrich) and ultrapure milli-Q water as titanium and oxygen precursors, respectively. The nominal thickness of the shell layer was estimated from x-ray reflectivity (XRR) measurements and SEM analysis.

Both monolayer and multilayer (3D colloidal crystals) configurations were prepared: in the first case, prior to ALD deposition, only one layer of SiO_2 microsphere was deposited on Si-wafer substrates, through self-assembly and evaporation of a diluted SiO_2 microspheres aqueous suspension, while 3D colloidal crystals, composed of approximately 10 layers of stacked microparticles, were obtained through the controlled sedimentation of more concentrated aqueous suspension of silica

spheres. After the coverage with the TiO_2 shell, the samples were annealed in air at 715 °C for 4 h, with a heating rate of 5 °C/min, to induce crystallization of the TiO_2 shell.

2.2. Preparation of PDA-Trex

PDA-Trex were obtained by coating the T-rex surface with a layer of polydopamine (PDA). The auto-polymerization of dopamine hydrochloride (DA) in a weakly alkaline solution was exploited. The reaction was carried out by dissolving dopamine hydrochloride (purchased by Merck) with a concentration of 2 mg/ml in a 25 mM tris (hydroxymethyl)aminomethane(TRIS)-buffer (purchased by Merck) solution (pH = 9.0). T-rex substrates were submerged in the DA solution, maintained under magnetic stirring to prevent the formation of a PDA film on the surface of the reaction solution and uncontrolled deposition on the T-rex surface. The final thickness of a PDA layer was varied testing different incubation times: 10 min–4 h. Analogous PDA-depositions were performed on Si wafers and quartz pieces.

2.3. Characterization of T-rex and PDA-Trex substrates

Morphological analysis of the developed SERS substrates was performed through Scanning Electron Microscopy (SEM) and Atomic Force Macroscopy (AFM). SEM analysis was performed by using a Phenom Pro Desktop scanning electron microscope (Thermo Fisher Scientific Inc., Eindhoven, the Netherlands), at an accelerating voltage of 15.0 kV, after coating the samples with 5 nm of Au.

AFM analysis was performed by using a NT-MDT NTEGRA (Limerick, Ireland) instrument, to evaluate surface morphology and roughness. Furthermore, AFM analysis was performed in contact mode on flat Si wafers after their incubation with DA alkaline solution to estimate the thickness of the deposited PDA layer.

Optical properties of the PDA coating layers and the developed substrates were evaluated using a Perkin-Elmer Lambda 900 UV–VIS–NIR Spectrometer (absorbance spectra on quartz substrates) and a QE 65000 Ocean Optics UV–VIS-NIR Spectrometer (reflectance spectra on T-rex monolayers).

The spectroscopical features proper of (PDA)-Trex substrates were

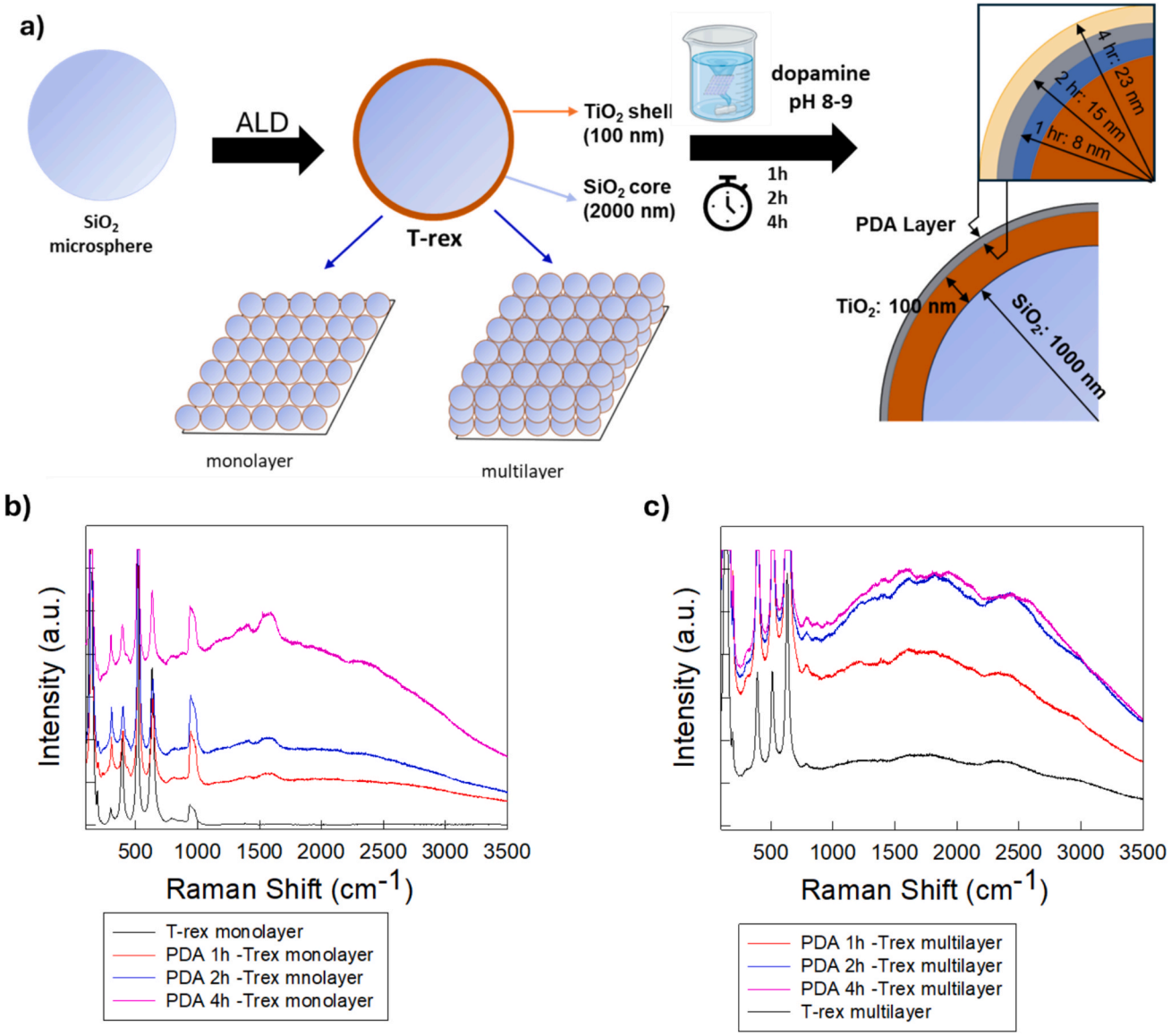

Fig. 1. a) Scheme of the preparation of the different types of PDA non-plasmonic SERS substrates; b) Raman spectra of pristine T-rex monolayer and PDA-Trex monolayers, with different PDA thickness (acquisition time, a.t. = 20 s); c) Raman spectra of pristine T-rex multilayer and PDA-Trex multilayers, with different PDA thickness (acquisition time, a.t. = 5 s).

investigated through Raman spectroscopy, using a Labram HR-800 μ-spectroscope (Horiba/Jobin-Yvon, using a He-Ne laser (λ = 633 nm) as exciting source and a 100X objective, N.A.: 0.9).

The surface wettability of the substrates was investigated using an Ossila (Leiden, NL) contact angle goniometer. The average contact angles were calculated from six different testing spots on each substrate.

2.4. SERS detection of methylene blue and histamine

Methylene Blue (MB) and Histamine (His) stock solutions with a concentration of 10^{-2} M were prepared by dissolving the appropriate amount of MB and histamine dihydrochloride (purchased by Merck) in 10 ml of Milli-Q water. Then, dilution was performed to achieve standard solutions with different concentrations in the range 10^{-8}–10^{-2} M. 20 μL of each of these solutions was deposited on T-rex and PDA-Trex substrates, and the droplets were left to evaporate in ambient conditions.

The substrates were analysed with the Labram HR-800 μ-spectroscope (Horiba/Jobin-Yvon, using as a He-Ne laser (λ = 633 nm) exciting source and a 100× objective, N.A.: 0.9).

At least 10 different points were measured for each sample.

Background was corrected to eliminate the fluorescent contribution, with the exception of data reported in Fig. 1b and c.

2.5. DFT simulation of the PDA-histamine and TiO_2-histamine interaction

Density Functional Theory (DFT) simulations were conducted with Quantum Espresso (http://www.quantum-espresso.org) as the periodic nature of plane-waves (PW) helps in representing infinite replicas of a single or a group of monomers. Further details can be found in SI 7.

3. Results and discussion

To obtain the PDA-functionalized non-plasmonic SERS substrates, we created dielectric core/shell structures by depositing, through ALD, 100 nm of TiO_2 on spherical SiO_2 microparticles (diameter of 2 μm) laying on Si-wafer substrates, both in the configuration of a monolayer or a 3D colloidal crystal. The two batches of samples were called T-rex monolayer and T-rex multilayer, respectively. Subsequentially, an overcoating layer of PDA was deposited on the T-rex surface by submerging them in an alkaline solution of dopamine hydrochloride and exploiting the auto-polymerization reaction of DA which occurred at ambient conditions (Fig. 1a). Different incubation times (10 min–4 h) were tested to control the final thickness and morphology of the overcoating PDA layer, with the aim of obtaining a thin PDA layer which homogeneously covered the external T-rex surface, without losing the spherical morphology, which has been demonstrated to be fundamental to maximize their performances during SERS experiments.[2] The same incubation processes with DA solution were performed on flat Si-wafers and the thickness of the obtained films was determined by scratch analysis through Atomic Force Microscopy in contact mode, revealing that 8 ± 1 nm, 15 ± 1 nm and 23 ± 3 nm – thick layers were obtained after 1, 2 and 4 h of incubation, respectively. The same thickness is assumed to be deposited on T-rex substrates. AFM investigation on incubated T-rex monolayers showed that the incubation with DA solution led to the formation of PDA NPs, whose number and aggregation increased as a function of incubation time (Fig. S1.1). Similarly, by increasing the incubation time, surface roughness gradually increased, passing from 0.768 nm for pristine T-rex to 1.250 nm, 1.357 nm and 1.972 nm for incubation times of 1 h, 2 h and 4 h, respectively (Fig. S1.2). The formation of these NPs aggregates on the external surface of the T-rex was confirmed also by SEM analysis (Fig. S1.3), as well as the retention of the T-rex spherical morphology.

Unfortunately, the direct AFM investigation of samples incubated for less than 1 h was not straightforward, due to the inherent surface roughness of PDA, and the limitations of AFM resolution at low thicknesses.

The effectiveness of the coverage of the T-rex surface by PDA layers also at low times of incubation, was demonstrated through UV–vis spectroscopy.

In Fig. S1.4 the UV–vis absorbance spectra of quartz pieces incubated with DA solution together with the T-rex samples and flat Si-wafers for 10 min, 20 min, 40 min, 1 h, 2 h and 4 h are reported. As a consequence of the incubation, the proper optical features of PDA (a main and broad absorption peak in the UV range and a less intense absorption tail in the visible range) appeared in the recorded spectra. As expected, the intensity of these spectral features regularly increased as a function of the incubation time. In particular, we used these data to estimate the thicknesses of the PDA coating for shorter polymerization times by measuring the optical density (OD) of the films at 400 nm. These OD values were then extrapolated using a polynomial fit derived from the OD vs. thickness data obtained for measurable PDA layers (60–360 min) and the resulting estimated thicknesses are 1.8 nm for 10 min, 4.3 nm for 20 min and 6.3 nm for 40 min. However, such short incubation times (<1 h) are likely to result in sparse and non-uniform PDA coatings, which are unsuitable for ensuring consistent analyte–surface interactions and reproducible SERS performance. For this reason, we focused our further investigation on T-rex samples incubated in dopamine solution for at least 1 h.

Reflectance measurements were performed directly on T-rex monolayer samples incubated with dopamine hydrochloride solution for 1–4 h (Fig. S1.5). The reflectance spectrum of the pristine T-rex monolayer was characterized by the presence of Fabry-Perot interference peaks, which gradually shifted to higher wavelengths, by increasing the thickness of the PDA layer (which led to a gradual increase of the refractive index of the surrounding medium).

The Raman spectra of T-rex (both in the case of monolayer and multilayer configurations, shown in Fig. 1b-c) were characterized by the presence of the peaks proper of TiO_2 anatase: the $E_{g(1)}$ mode at 143 cm^{-1}, the $E_{g(2)}$ mode at 192 cm^{-1}, the $A_{1g+B1g(2)}$ at 390 cm^{-1} and the $E_{g(3)}$ mode at 632 cm^{-1}. In the case of T-rex monolayer, the Raman signals of the underlying Si substrates were still clearly visible at 301 cm^{-1}, 520 cm^{-1} and 940 cm^{-1}, while in the case of T-rex multilayer only the main Si peaks at 520 cm^{-1} was still visible. This observation confirmed that in this configuration the laser did not reach completely the underlying substrate, but it was entrapped inside the 3D colloidal crystal structure, in accordance with our previous studies. [2,8,9].

Additional peaks were visible, especially in the case of the multilayer configuration, at 1282 and 1388 cm^{-1}, and they are ascribable to the CO_2 adsorbed on the T-rex surface.[3].

The overcoating with PDA layers induced significant modifications in the Raman spectra, with an increase of the fluorescence background and the appearance of two broad peaks at 1409 and 1575 cm^{-1}, which are typical of amorphous carbonaceous species. These spectral features are in agreement with what observed in other research works related to PDA [37]. The 1409 cm^{-1} peak, in fact, is ascribable to the D band due to disordered C atoms, while the 1575 cm^{1} peak is ascribable to the G band, proper of graphitic C atoms.

The chemical structure of PDA is formed through the oxidation of dopamine's catechol group, producing 5,6-dihydroxyindole and 5,6-indolequinone monomers, which then undergo further oxidation and coupling reactions. Some reactions generate oligomers that aggregate through supramolecular interactions, such as hydrogen bonding, π–π stacking, and van der Waals forces, while others, driven by free radical intermediates, form carbon–carbon bonds between adjacent aromatic rings, leading to the formation of polycatecholamine products. [38] As a result, PDA exhibits a complex and heterogeneous structure, characterized by both ordered and disordered aromatic domains, which are clearly revealed through Raman analysis. Interestingly, in PDA-Trex substrates both the intensity of the fluorescence background and of the two C-related bands increased proportionally to the incubation time and PDA thickness. In particular, the baseline at 1055 cm^{-1} (a

wavenumber chosen for the absence of any real Raman peak) for an acquisition time of 20 s rose from ~120 counts for the bare T-rex monolayer, to ~10580 counts for the PDA 1 h-Trex monolayer, ~16436 counts for the PDA 2 h-Trex monolayer and ~39741 counts for the PDA 4 h-Trex monolayer. In the case of T-rex multilayers, a less linear trend was observed, with a significant increase of the fluorescence background after only 1 h of incubation with the DA alkaline solution (passing, for an qcquisition time of 5s, from ~14307 counts for the bare T-rex multilayer to ~37749 counts for the PDA 1 h-Trex multilayer), and small differences between T-rex multilayers incubated for 2 h and 4 h (~46625 counts and ~50060 counts, respectively). This is probably due to the fact that only the upper few (3–4) layers of the 3D colloidal crystal were covered by PDA nanostructures, as indicated by SEM investigation reported in Fig. S1.6. Despite T-rex colloidal crystals can work as sponge and get infiltrated by solutions, it is probable that DA self-polymerization occurred before DA monomers could completely diffuse inside the whole 3D structure of T-rex multilayers. On the other hand, the addition of an overcoating layer of PDA to multilayers T-rex led to a more significant increase in the fluorescence background of the Raman spectra, entailing the need of limiting the acquisition time of the measurements to only 2–5 s. Unfortunately, this fact could decrease the success of further SERS detection of analytes.

These results demonstrated that the incubation of T-rex with dopamine solution is an extremely simple strategy to introduce on the TiO_2 surface an additional layer of an adhesive and rich of conjugated double bonds material, without the need of any surface preparation or sophisticated synthesis procedures, by simply exploiting the good adhesiveness of PDA on a large variety of materials. In the specific case of an underlying TiO_2 layer, H-bonds can be formed, leading to a close binding which results in a stable coverage.[39].

Then, we verified the effect of the addition of this PDA layer on the SERS activity of the T-rex, similarly to what was observed in literature in the case of all-plasmonic or hybrid SERS substrates. To achieve this, we treated the substrates with varying concentrations of methylene blue (MB), an organic dye known for its strong and well-defined Raman signature, particularly when excited with a 633 nm laser. MB exhibits an intense and broad optical absorption band in the 550–700 nm range, with a maximum at 664 nm. As a result, the excitation wavelength used for Raman analysis lies within the electronic absorption band of MB, leading to resonance conditions that enhance its Raman signal. However, this signal can be further enhanced in presence of SERS substrates (Fig. S2). Fig. 2a and b show a comparison between the Raman spectra of MB solutions (concentration range 10^{-6} – 10^{-4} M) obtained using as SERS substrates pristine T-rex or PDA 2 h-Trex monolayers and a MB 10^{-3} M solution deposited directly on a Si wafer (in absence of any SERS substrate).

First of all, in accordance with previous works [1–3,9,40], it is visible that T-rex monolayers are capable to work as SERS substrates and increase the MB Raman signal.

More interestingly, it is evident that the addition of a PDA 2 h overcoating layer enhanced the detection of MB by T-rex monolayers, both enhancing the intensity of the Raman peaks proper of the organic dye and lowering the detection limit (Fig. 2a–e).

The calculated enhancement factor (EF, *see* Supporting Information SI 2 for calculation details) for pristine T-rex monolayer was limited to 25, while it increased to 840 after the addition of the PDA overcoating layer. These values are in line with the values of EF conventionally obtained for non-plasmonic SERS substrates, usually in the order of 10^2-10^3, while they are lower than those conventionally obtained for plasmonic SERS substrates (*see* Table S1). For example, Yuan et al. reported an EF of ~10^7 for MB employing as SERS substrates Au Nanoworms conjugated with MoS_2 thanks to PDA. [20] Similarly, even if Schiavi et al. did not calculate the EF achieved during the detection of MB using silver nanoparticles with nanometric coating of polydopamine, they could achieve a lower detection limit (0.025 μM instead of 1 μM). [26].

However, the obtained values of EF clearly demonstrate that PDA can enhance the SERS activity of T-rex monolayers in the case of MB.

Furthermore, with pristine T-rex monolayer MB could be detected starting from a concentration of 10^{-5} M, while using PDA 2 h-Trex monolayer the detection limit was extended to 10^{-6} M. The improved detection of MB thanks to PDA coating can be due to the chemical structure of PDA rich in aromatic rings and conjugated π structures, which can maximize the interactions with the organic structure of the dye, particularly through π–π stacking. Furthermore, thanks to the presence of various phenolic group, which can be partially deprotonated in operating conditions, PDA nanostructures exhibit a negative surface charge [41] that can attract positively charged analytes [42,43], such as cationic dyes like MB, promoting their preconcentration and improving their detection (Fig. 2f). So, PDA can enhance the affinity between the dye molecules and the SERS substrate surface, leading to better detection and signal intensity.[26].

As illustrated in Fig. 2, the 2 h PDA overcoating layer exhibited a consistent positive effect across all tested MB concentrations, resulting in a constant increase in the intensity of all MB-associated Raman peaks.

Subsequently, we investigated the effect of the variation of the incubation time (and related PDA thickness) on the SERS performances of PDA-Trex monolayers. Fig. 3a reports a comparison between the average Raman spectra for MB 10^{-6} M obtained using T-rex monolayers incubated with DA solutions for 1 h, 2 h or 4 h. Fig. 3b further elaborates the same data in the form of histogram (representing the average value of 10 experimental measurements recorded in 10 different points inside the same substrate. Error bars represent the calculated standard deviation) considering the intensity at 1620 cm^{-1} (assigned to C–C/C–N stretching), which can be considered as the most representative peak for the MB molecule. For all PDA-Trex monolayers the intensity of the peak at 1620 cm^{-1} was significantly increased in the presence of MB 10^{-6}M, with a clear, distinct peak appearing, confirming that the organic dye can be detected starting from this concentration. Furthermore, Fig. 3a and b demonstrate that, at the 10^{-6}M concentration, the PDA 4 h- Trex monolayer delivered the best performance.

A similar analysis was performed for the MB 10^{-5} and 10^{-4} M solutions, and the results are summarized in histograms reported in Fig. 3c–d. As with the 10^{-6} M solution, all PDA-Trex monolayers, independently of the incubation time, outperformed pristine T-rex monolayers. However, for MB 10^{-5} and 10^{-4}M solutions, slightly better performances could be achieved with the PDA 2 h-Trex monolayer, rather than with PDA 4 h-Trex monolayer.

The exact reason for this slightly variable behavior of the SERS performance as a function of incubation time is still under investigation. On one hand it must be underlined that the difference between the SERS performances is quite limited, on the other hand it must be considered that beyond mere chemical intermolecular interactions— enhanced by a thicker PDA layer due to the increased availability of functional groups— additional effects may play a significant role in maximizing the SERS effect. An example is represented by variations in surface wettability: an increase in the hydrophobicity of the SERS substrate surface, in fact, can cause aqueous solutions to concentrate in a more confined area, thereby enhancing the detection of dissolved analytes. To investigate this effect, we analyzed changes in the surface wettability of T-rex monolayers after the deposition of increasing amounts of PDA, with the results presented in Fig. S3.

As expected, PDA deposition on a TiO_2-coated Si wafer increased surface hydrophilicity, regardless of the PDA thickness. This can be attributed to the exposed hydrophilic groups, including hydroxyl (–OH) and amino ($–NH_2$) groups on the surface of the PDA nanolayer. The contact angle trend went from approximately 95° for pure silicon, to around 65° for TiO_2-coated Si wafer, and further decreased to about 50° for PDA, consistent with previously reported data. [44,45].

On the other hand, T-rex monolayers exhibited less defined behavior. Pristine T-rex had slightly lower contact angle values (~60°) than the TiO_2-coated Si wafer, and these values remained around the same value after 1-hour and 2-hour PDA coating. Only the thicker PDA nanolayer (4

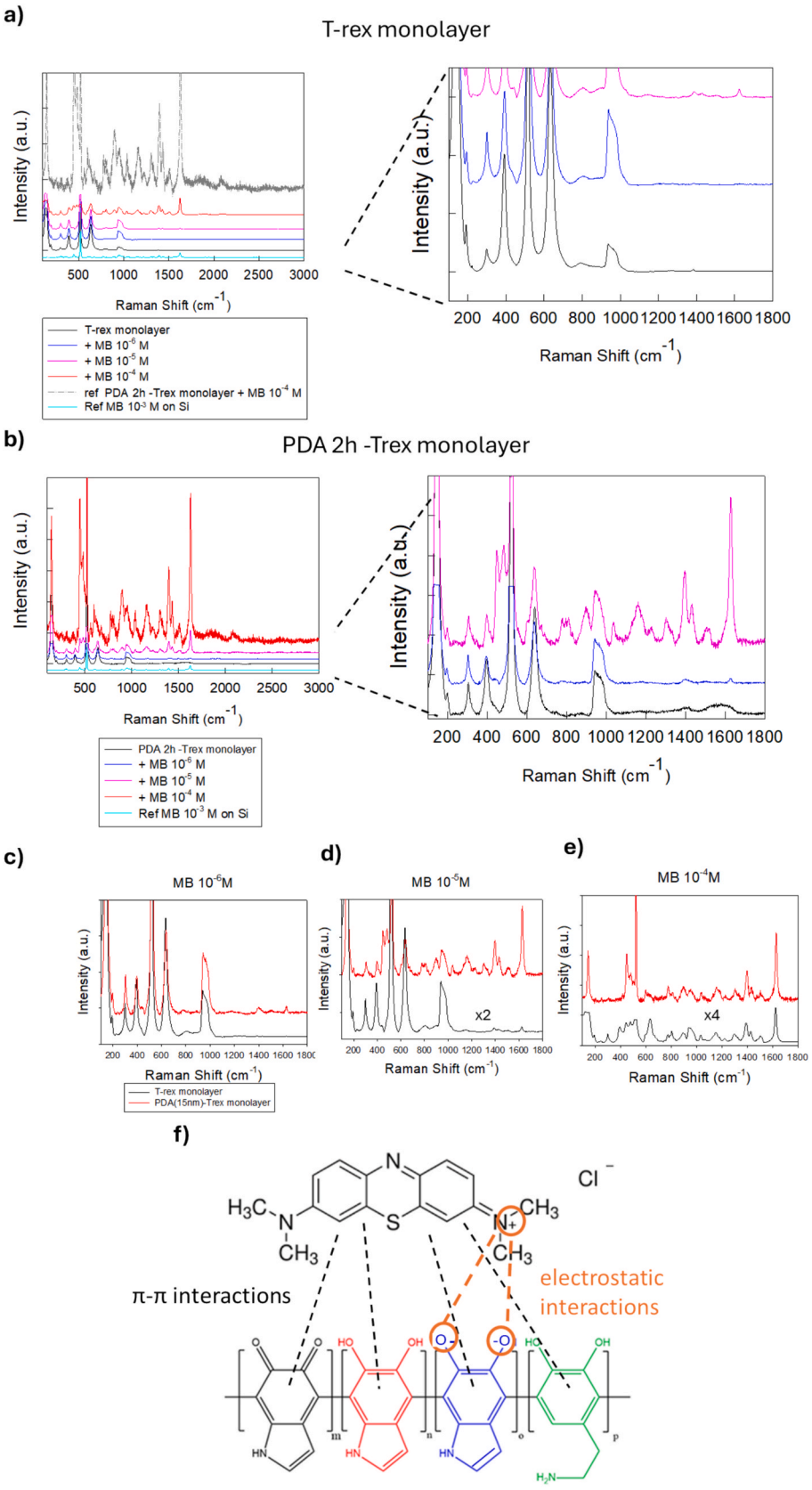

Fig. 2. a) Raman spectra of MB at different concentrations in presence of pristine T-rex monolayer (acquisition time: 20 s) and zoom on the spectra for lower concentrations; b) Raman spectra of MB at different concentrations in the presence of PDA 2 h-Trex monolayer (acquisition time: 20 s) and zoom on the spectra for lower concentrations; c) direct comparison between the Raman spectra of MB 10^{-6} M using T-rex monolayer or PDA 2 h-Trex monolayer; d) direct comparison between the Raman spectra of MB 10^{-5} M using T-rex monolayer or PDA 2 h-Trex monolayer; e) direct comparison between the Raman spectra of MB 10^{-4} M using T-rex monolayer or PDA 2 h-Trex monolayer; f) scheme of possible interactions between PDA and MB.

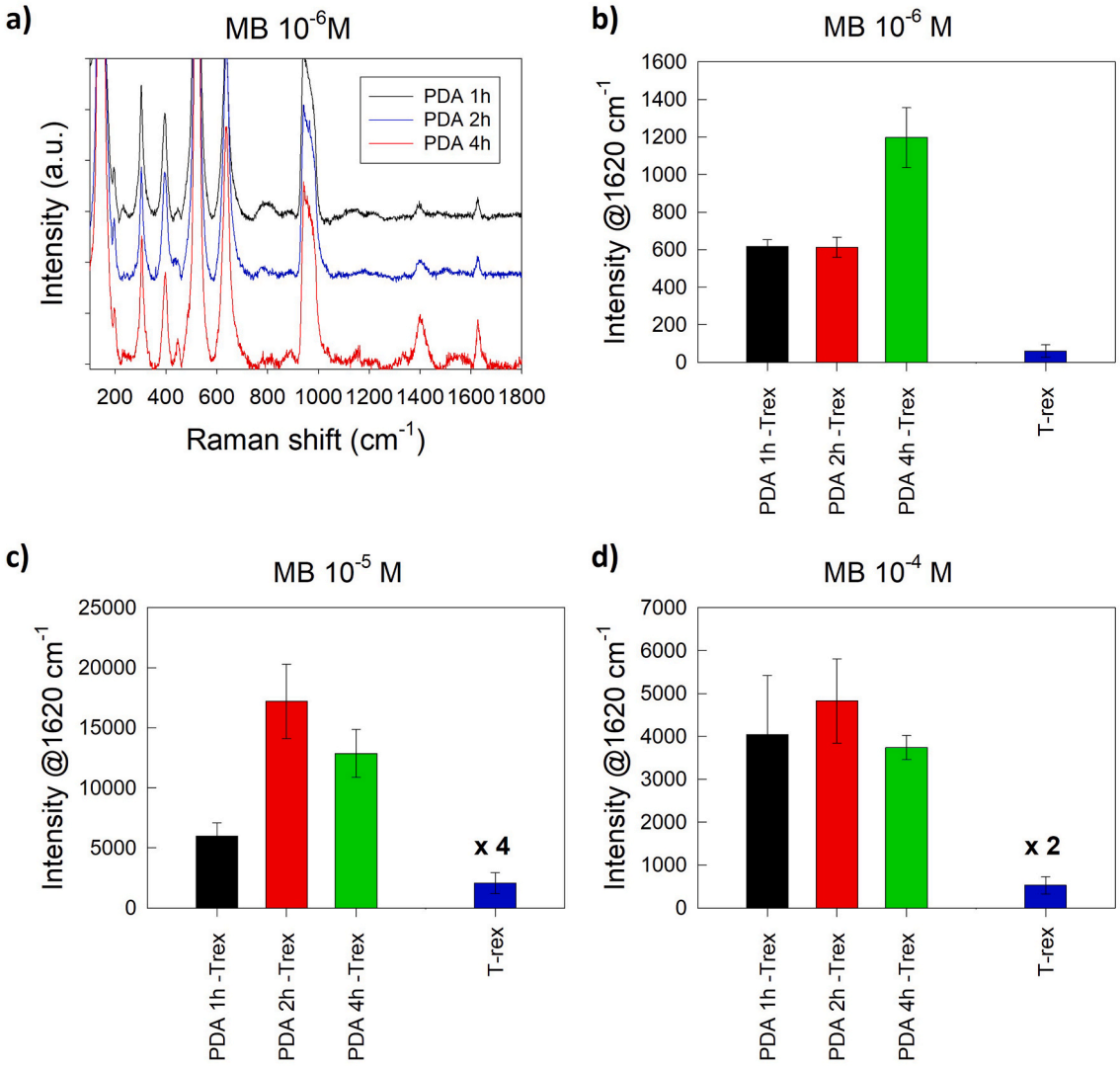

Fig. 3. Comparison between the SERS performances of T-rex monolayers with PDA overcoating layers with different thickness. a) Comparison between the Raman spectra of MB 10^{-6} M (a.t. 10 s); b) comparison between the intensity of the peak at 1620 cm^{-1} for MB 10^{-6} M (a.t. 10 s); c) comparison between the intensity of the peak at 1620 cm^{-1} for MB 10^{-5} M (a.t. 10 s); d) comparison between the intensity of the peak at 1620 cm^{-1} for MB 10^{-4}M (a.t. 1 s, filter 50 %). Error bars represent the standard deviation calculated from measurements taken at 10 different locations on the same substrate.

h) showed a clear differentiation, resulting in a further increase in surface wettability (~45).

The collected data suggest that the difference in SERS performances of PDA nanolayers with varying thicknesses is more related to chemical intermolecular interactions than to variations in surface wettability.

Additionally, it has to be considered that the effect of the electromagnetic field enhancement performed by a SERS substrate and felt by adsorbed analyte molecules gradually decreases moving away from the substrate surface: even if this effect is significantly stronger in the case of plasmonic substrates (where the distance between the SERS surface and the analyte should be limited within less than 8 nm [26]) rather than in the case of non-plasmonic substrates [46], the deposition of a thick PDA layer on the external surface of the T-rex could be detrimental and minimize this effect. Furthermore, increasing the incubation time and PDA layer thickness affected the intensities of the D and G bands characteristic of PDA in the Raman spectra, as well as the background fluorescence. This fact, in turn, imposed limitations on acquisition times, making the detection of analytes at low concentrations more challenging. This effect was particularly evident in the case of multilayer substrates.

Pristine T-rex 3D colloidal crystals enabled a better detection of MB in comparison to monolayer counterparts, for all the tested concentrations (Fig. S4a), in line with what observed in our previous work.[2] The reason is that they can entrap light inside the structure of the colloidal crystal, giving origin to multiple light scattering not only inside the single sphere, but also between the different spheres of the crystal.[2] In the case of PDA-Trex, instead, we observed a less regular trend, especially in correspondence of higher PDA thickness (Figs. S4b-4d). This can be due, again, to two different processes: on one hand, thicker PDA layers may spatially separate the analyte from the SERS surface, reducing the SERS enhancement; on the other hand, prolonged polymerization times can result in thicker coatings with a more extended conjugated structure, which can increase intrinsic fluorescence under visible excitation. During our experiments we were forced to repeat the acquisition on the same point more times before acquiring a signal which did not saturate the detector of the Raman spectrometer or to reduce the acquisition times, with a significant lowering of the intensities of the recorded MB peaks and a reduction of the ease and immediacy of the analysis.

Fluorescence is one of the main competing optical processes that can interfere during a Raman analysis, and it can be a serious problem for the analysis of systems containing conjugated or aromatic structures,

like PDA. It is well known that this effect often represents a major challenge for the sensitivity and reliability of Raman-based detection, and the individuation of innovative strategies for this limitation is out of the scope of this work. However, several technical strategies to minimize this fluorescence interference could be implemented in future studies, being fundamental to extend the utilization of the PDA-Trex substrates to a wide range of analytes and measurement conditions. For example, the adoption of Raman instruments with fluorescence suppression modules (i.e. time-gated detection, shifted excitation Raman difference spectroscopy (SERDS), or modulated laser sources) could enable the use of thicker PDA layers or T-rex multilayers without compromising spectral quality.[47,48] Other strategies could involve the utilization of alternative (in the near infrared range) excitation wavelengths, the addition of fluorescence quenchers (i.e. graphene, graphene oxide..) [44], or the optimization of synthetic procedures to obtain uniform ultrathin (<2 nm) PDA coatings. Achieving such homogeneous films could not only limit fluorescence background, but also promote the formation of an S-scheme heterojunction between PDA and TiO_2, enhancing charge separation and charge transfer processes, [39] thereby further increasing the SERS activity through a chemical enhancement effect.

For all these reasons, PDA 2 h-Trex monolayer was considered the best non-plasmonic SERS substrate among the tested ones, with a good balance between the enhancement of the Raman signal and the convenience of use.

The uniformity, long-term stability, and reusability of this substrate were evaluated using a 10^{-4} M MB solution, as reported in Fig. S5.

Fig. S5a shows a comparison of eleven Raman spectra acquired under identical conditions (1 s acquisition time, f50%) at eleven different locations on the same SERS substrate. The calculated relative standard deviation (RSD) of the main MB peak intensity was 14 %. This value is higher than that typically observed for pristine T-rex monolayers (~4%, as reported in [9]), likely due to slight variations in the thickness and spatial distribution of the PDA layer, which may lead to non-uniform interactions with the analyte. Even higher standard deviation values were observed for other MB concentrations and PDA coatings, as shown by the error bars in the histograms of Fig. 2.

The temporal stability of the substrate was also investigated, as shown in Figs. S5b and S5c. In standard storage conditions (i.e., ambient temperature and atmosphere, no laser exposure), the substrate exhibited good stability over a period of 10 months. As reported in Fig. S5b, the intensity of the MB peak at 1620 cm^{-1} decreased by only 1.3 % after the first week, ~8% after one month, and ~17 % after ten months. However, it should be noted that it is difficult to clearly distinguish between substrate degradation and the spontaneous degradation of the analyte, as both likely contribute to the observed decrease in signal intensity over time.

The substrate stability under measurement conditions was assessed by repeatedly acquiring Raman spectra at the same location over time (Fig. S5c). A progressive decrease in the MB signal was observed, probably due to the occurrence of a self-photodegradation process. In fact, upon visible irradiation under resonant conditions, MB is photoexcited and generates singlet oxygen species. These are strong oxidizing agents which can act against MB itself and promote self-degradation (photobleaching). This process can be catalyzed by the TiO_2 shell present in the T-rex structure.

Finally, the reusability of the PDA 2 h-T-rex monolayer was tested, as shown in Fig. S5d. The same substrate was used for three consecutive detection cycles of 10^{-4} M MB. After each measurement, the deposited MB was removed by exposing the substrate to ozone in a UV-cleaner for 400 min. A fresh MB drop was then applied and analyzed under the same experimental conditions. A slight decrease in performance was observed across the three cycles: the intensity of the main MB peak decreased by ~ 13 % from the first to the second cycle, and by ~ 21.5 % from the first to the third cycle.

The PDA 2 h-Trex monolayer was further tested for the detection of histamine, an organic nitrogenous compound whose chemical structure is reported in Fig. 4a.

Examples of the Raman spectra recorded when a drop of histamine solution (concentration range: 10^{-8} M-10^{-2} M) was deposited on the PDA 2 h-Trex monolayer are reported in Fig. 4b. This SERS substrate enabled the detection of histamine starting from the 10^{-8} M concentration, showing the appearance of various distinct peaks in the 850–1450 cm^{-1} spectral range, which gradually increased with the increase of the histamine concentration passing from 10^{-8} M to 10^{-4} M. For higher concentrations, instead, no further increase (or even a decrease) in the intensity of the Raman peaks was observed (Fig. 4b-c), in line with what observed with other SERS substrates. In fact, only molecules adsorbed near the surface of the substrate can take advantage from its SERS effect and the signal normally saturates at high concentrations.

Histamine detection was also performed using pristine T-rex monolayers, and the corresponding spectra at different concentrations are shown in Fig. 4 e-f. The detection limit passed to 10^{-7} M, when very weak signals were observed only in areas where crystalline aggregates were visible under the microscope coupled with the Raman spectrometer, as evidenced by larger standard deviation. Even at high histamine concentrations, detection with pristine T-rex was possible only in the presence of these precipitates, further highlighting the beneficial effect of the PDA overcoating layer in enhancing the performance of T-rex substrates.

Furthermore, if we compare the Raman signals obtained in presence of the T-rex monolayer with those of a drop of histamine solution 10^{-2} M directly deposited on the Si substrate in absence of a SERS enhancer (green line in Fig. 4e), we can notice the suppression of some of the Raman peaks and the appearance of new ones in the SERS spectrum. The interpretation of the Raman peaks of the histamine free solution is reported for convenience in Table S1. Even if the unambiguous attribution of the new peaks in SERS spectrum is out of the scope of this paper, it is evident that the main modifications regarded vibrations of the imidazole ring, which were probably highly perturbed by the interaction on the Trex surface (particularly evident is the suppression of the peak at 1570 cm^{-1} ascribable to imidazole ring stretching). In fact, different theoretical studies demonstrated that the imidazole ring is the main responsible of the adsorption of histamine or histidine on TiO_2 surfaces [49]. This conclusion is further supported by DFT simulations, as reported in SI7 and in Fig. 4g, where H bonds formed between the TiO_2 anatase surface and the histamine molecule are represented.

These variations in the SERS spectrum were further emphasized when PDA 2 h-Trex monolayer was considered, suggesting that at the basis of the enhancement of efficiency in the SERS detection there was the insurrection of stronger intermolecular interactions, as demonstrated by Fig. 4d and SI 7. In particular, H-bonds can form between the different donor or acceptor sites present in histamine and PDA chemical structures. For example, as reported in Fig. 4d, the hydrogen atom of the secondary amine in polydopamine can act as a hydrogen bond donor, interacting with the lone pair of the nitrogen atom in the primary amine group of histamine (*see* SI 7 for details on other possible PDA-histamine interactions). Additionally, aromatic rings in the PDA structure could interact through π–π forces with the double bonds of the imidazole ring proper of histamine or the quinone groups in the PDA structure could react with the amine group contained in histamine through Michael addition and/or Schiff base reactions [23,27,50], as suggested by the disappearance of the N–H stretching peaks at 3100 cm^{-1}(Fig. S8). Furtherly, electrostatic interactions between the negative PDA nanostructures and the positively charged monocationic and free base histamine (which are the main species for histamine hydrochloride present in milli-Q water [51]) could occur. All these possible interactions lead to a stronger adsorption of histamine on PDA rather than a TiO_2 surface. According to our DFT simulations, in fact, the adsorption of histamine on the (101) TiO_2 surface (the most stable in the case of anatase), is characterized by an adsorption energy of –37 kJ/mol, which decreases to ~ -48 kJ/mol in the case of PDA. Experimental evidence

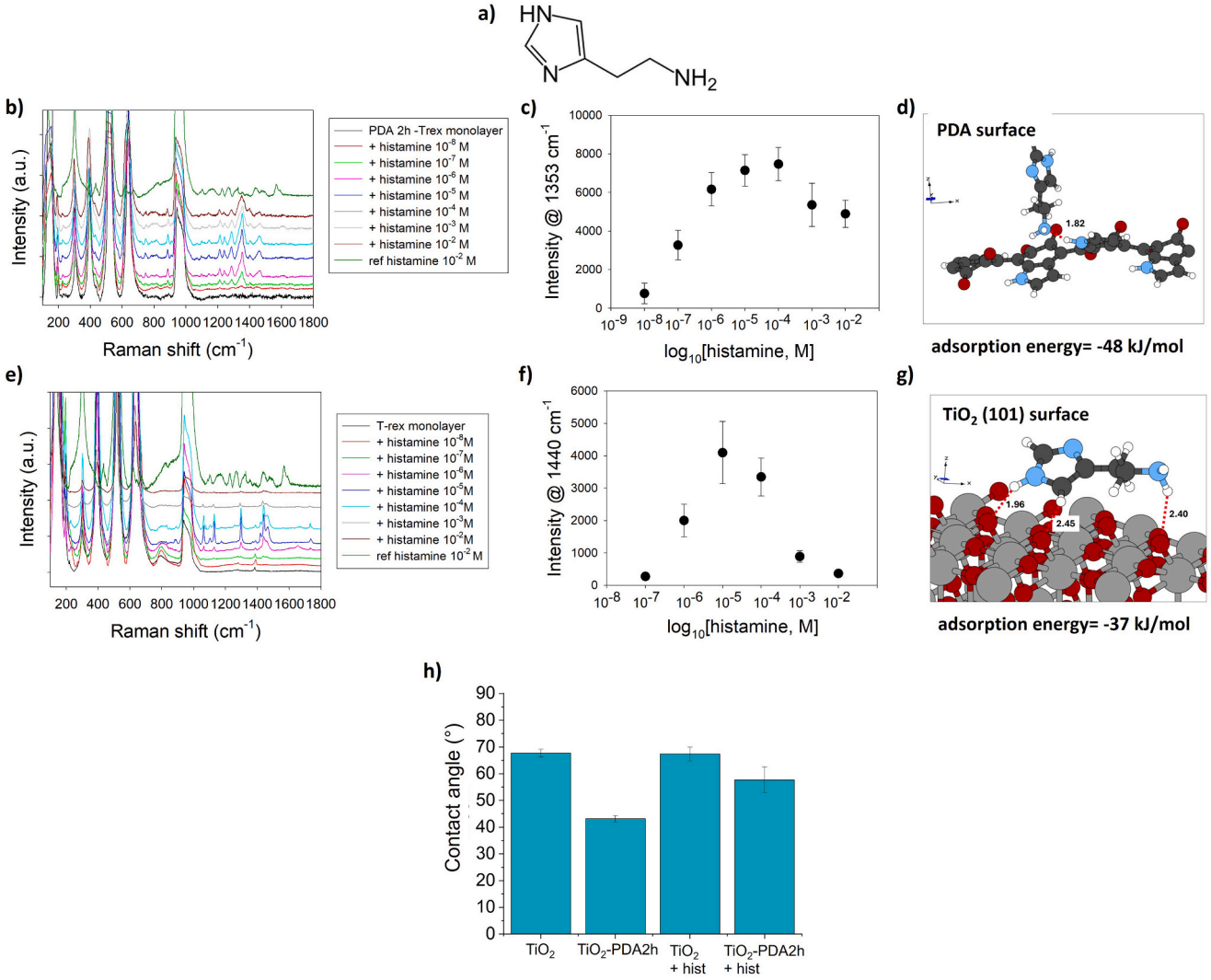

Fig. 4. Histamine detection. a) Chemical structure of histamine; b and e) SERS spectra of histamine (10^{-8}-10^{-2} M) using PDA 2h-Trex monolayer (b) or pristine T-rex monolayer (e) as SERS substrates and comparison with the conventional Raman spectrum of a concentrated (10^{-2} M) histamine solution on a Si substrate (dark green line). Acquisition time 30 s; c) and f) correspondent variations of the intensity of the main histamine peak as a function of its concentration; d) and g) results of the DFT simulations for the adsorption of histamine on a PDA surface or TiO_2 (101) surface, respectively; h) variation of the contact angle values of a TiO_2-coated Si wafer and a PDA 2 h−TiO_2-coated Si wafer before and after histamine adsorption.

also supports a stronger interaction between histamine and PDA compared to TiO_2, as demonstrated by contact angle measurements shown in Fig. 4h. The incubation of a TiO_2-coated Si wafer with a histamine 10^{-3} M solution for 2 h and subsequent washing with water did not lead to any significant modification of the contact angle value typical of the TiO_2 surface; on the contrary, when a PDA 2 h-TiO_2-coated Si wafer was incubated with the same histamine solution for the same period, the contact angle was increased by ~15°, demonstrating the decrease of the hydrophilicity of the surface as a consequence of the histamine adsorption.

All these complex interactions could lead to a variation of the molecular geometry and electronic structure of histamine, making evident the effect of the so-called SERS "chemical enhancement", which can add up to the electromagnetic enhancement effect and lead to lower detection limits. [17,19,20] Generally speaking, two different types of phenomenon can contribute to this effect also in the case of non-plasmonic SERS substrates [1,52,53]: the insurrection of charge (electrons) transfer processes between the analyte and the SERS substrate (according to the electronic structures of the involved chemical species, both substrate-to-analyte or analyte-to-substrate electron transfers are possible) or the modification of the analyte polarizability due to the immobilization of the molecule on a solid surface leading to the formation of a novel substrate-molecule complex. On one hand, PDA can effectively facilitate the anchoring of an analyte on the T-rex surface through the discussed intermolecular interactions, introducing a variation of the polarizability of the molecule; on the other, the conjugated π structure of PDA enriched by quinone or catechol groups, can be an ideal pathway for charge flow [40,52] between the underlying TiO_2 and histamine, making PDA an excellent electron transfer mediator. [17,54,55] Alessandri et al. [40] and Hurst et al. [52] demonstrated that the catechol group can be and excellent anchoring group on a TiO_2 surface, enabling the formation of an efficient charge-transfer complex. Catechol groups are present inside the PDA structure, together with aromatic rings, which can create further paths for electron transfer towards the adsorbed histamine molecules. These phenomena can contribute to the overall Raman enhancement and result in an easier detection of the organic analyte in comparison to pristine T-rex.

4. Conclusion

In this work, we investigated the impact of applying a thin layer of PDA on the surface of a non-plasmonic SERS substrate (T-rex) on their

capability to detect organic molecules.

Preliminary experiments focused on methylene blue (MB), a standard Raman probe, and demonstrated that the PDA coating promoted its surface adsorption via π–π and electrostatic interactions, increasing the T-Rex SERS activity by a factor of 10. The superior performance of PDA-functionalized T-rex substrates was confirmed also in the detection of histamine, a biogenic amine that can contaminate improperly stored or fermented food, potentially causing allergic reactions. In presence of the PDA coating, the detection limit for histamine was reduced by an order of magnitude (10^{-8} M compared to 10^{-7} M for pristine T-rex). Our results indicated that PDA not only facilitates analyte binding through H-bonding, but, in this case, it also contributes to a chemical enhancement mechanism, via analyte structure and polarizability alteration and charge transfer.

Overall, PDA functionalization represents a simple, fast, and scalable strategy to increase the sensitivity and stability of T-rex, offering a cost-effective route for the development of advanced alternative non-plasmonic SERS substrates.

CRediT authorship contribution statement

Autchariya Boontanom: Writing – review & editing, Visualization, Investigation, Data curation. **Leonardo Moscolari:** Writing – review & editing, Investigation. **Erika Kozma:** Writing – review & editing, Methodology, Investigation. **Michele Speziani:** Writing – review & editing, Visualization, Investigation, Data curation. **Ivano Alessandri:** Writing – review & editing, Methodology. **Francesco Galeotti:** Writing – review & editing, Visualization, Supervision, Project administration, Investigation, Funding acquisition, Data curation, Conceptualization. **Irene Vassalini:** Writing – original draft, Visualization, Supervision, Methodology, Investigation, Funding acquisition, Data curation, Conceptualization.

Declaration of competing interest

The authors declare that they have no known competing financial interests or personal relationships that could have appeared to influence the work reported in this paper.

Acknowledgement

We acknowledge financial support under the National Recovery and Resilience Plan (NRRP), Mission 4, Component 2, Investment 1.1, Call for tender No. 104 published on 2.2.2022 by the Italian Ministry of University and Research (MUR), funded by the European Union – NextGenerationEU – Project "PolyDOpamine funCTional surfaces for SERS monitORing of FOOD contamination (DrFOOD)" – CUP D53D23005520006 – Grant Assignment Decree No. 966 adopted on 30/06/2023.

Appendix A. Supplementary data

Supplementary data to this article can be found online at https://doi.org/10.1016/j.apsusc.2025.165249.

Data availability

Data will be made available on request.

References

[1] I. Alessandri, J.R. Lombardi, Enhanced Raman scattering with dielectrics, Chem. Rev. 116 (2016) 14921–14981, https://doi.org/10.1021/acs.chemrev.6b00365.
[2] I. Alessandri, Enhancing raman scattering without plasmons: unprecedented sensitivity achieved by TiO2 shell-based resonators, J. Am. Chem. Soc. 135 (2013) 5541–5544, https://doi.org/10.1021/ja401666p.
[3] N. Bontempi, L. Carletti, C. De Angelis, I. Alessandri, Plasmon-free SERS detection of environmental CO2 on TiO2 surfaces, Nanoscale 8 (2016) 3226–3231, https://doi.org/10.1039/c5nr08380j.
[4] I. Alessandri, N. Bontempi, L.E. Depero, Colloidal lenses as universal Raman scattering enhancers, RSC Adv. 4 (2014) 38152–38158, https://doi.org/10.1039/c4ra07198k.
[5] S. Cong, Y. Yuan, Z. Chen, J. Hou, M. Yang, Y. Su, Y. Zhang, L. Li, Q. Li, F. Geng, Z. Zhao, Noble metal-comparable SERS enhancement from semiconducting metal oxides by making oxygen vacancies, Nat. Commun. 6 (2015) 1–7, https://doi.org/10.1038/ncomms8800.
[6] N. Bontempi, I. Vassalini, S. Danesi, I. Alessandri, ZORRO: zirconium oxide resonators for all-in-one Raman and whispering-gallery-mode optical sensing, Chem. Commun. 53 (2017) 10382–10385, https://doi.org/10.1039/c7cc06357a.
[7] N. Bontempi, I. Vassalini, S. Danesi, M. Ferroni, M. Donarelli, P. Colombi, I. Alessandri, Non-Plasmonic SERS with silicon: is it really safe? New insights into the optothermal properties of core/shell microbeads, J. Phys. Chem. Lett. 9 (2018) 2127–2132, https://doi.org/10.1021/acs.jpclett.8b00662.
[8] I. Vassalini, O. Sisman, E. Comini, I. Alessandri, The role of morphology in all-dielectric SERS: a comparison between conformal (T-rex) and non conformal TiO2 shells, Vib. Spectrosc 109 (2020), https://doi.org/10.1016/j.vibspec.2020.103085.
[9] I. Alessandri, L. Carletti, M. Ferroni, C. De Angelis, I. Vassalini, Bioinspired self-similar all-dielectric antennas: probing the effect of secondary scattering centres by Raman spectroscopy, Mater. Adv. 1 (2020) 2443–2449, https://doi.org/10.1039/d0ma00509f.
[10] D. Chen, X. Zhu, J. Huang, G. Wang, Y. Zhao, F. Chen, J. Wei, Z. Song, Y. Zhao, Polydopamine@Gold nanowaxberry enabling improved SERS sensing of pesticides, pollutants, and explosives in complex samples, Anal. Chem. 90 (2018) 9048–9054, https://doi.org/10.1021/acs.analchem.8b01348.
[11] Z. Zhang, T. Si, J. Liu, K. Han, G. Zhou, Controllable synthesis of AgNWs@PDA@AgNPs core-shell nanocobs based on a mussel-inspired polydopamine for highly sensitive SERS detection, RSC Adv. 8 (2018) 27349–27358, https://doi.org/10.1039/c8ra04936j.
[12] D. Wang, L. Bao, H. Li, X. Guo, W. Liu, X. Wang, X. Hou, B. He, Polydopamine stabilizes silver nanoparticles as a SERS substrate for efficient detection of myocardial infarction, Nanoscale 14 (2022) 6212–6219, https://doi.org/10.1039/d2nr00091a.
[13] B. Shang, Y. Wang, P. Yang, B. Peng, Z. Deng, Synthesis of superhydrophobic polydopamine-Ag microbowl/nanoparticle array substrates for highly sensitive, durable and reproducible surface-enhanced Raman scattering detection, Sensors Actuators, B Chem. 255 (2018) 995–1005, https://doi.org/10.1016/j.snb.2017.07.194.
[14] J. Dong, T. Wang, E. Xu, F. Bai, J. Liu, Z. Zhang, Flexible hydr0ophobic CFP@PDA@AuNPs stripes for highly sensitive SERS detection of Methylene Blue residue, Nanomaterials 12 (2022) 1–13, https://doi.org/10.3390/nano12132163.
[15] J. Du, C. Jing, One-step fabrication of dopamine-inspired Au for SERS sensing of Cd 2+ and polycyclic aromatic hydrocarbons, Anal. Chim. Acta 1062 (2019) 131–139, https://doi.org/10.1016/j.aca.2019.02.033.
[16] J. Wang, Y. Yang, H. Li, J. Gao, P. He, L. Bian, F. Dong, Y. He, Stable and tunable plasmon resonance of molybdenum oxide nanosheets from the ultraviolet to the near-infrared region for ultrasensitive surface-enhanced Raman analysis, Chem. Sci. 10 (2019) 6330–6335, https://doi.org/10.1039/c9sc02202c.
[17] L. Tan, Y. Cao, J. Yan, K. Mao, L. Liu, X. Wang, W. Ye, R.A. Harris, H. Zhang, TiO2 nanorod arrays@PDA/Ag with biomimetic polydopamine as binary mediators for duplex SERS detection of illegal food dyes, Anal. Chim. Acta 1287 (2024) 342047, https://doi.org/10.1016/j.aca.2023.342047.
[18] S. Pekdemir, Polydopamine-mediated facile silver grown on ZnO thin films as high performance SERS substrates for R6G detection, Cumhur. Sci. J. 45 (2024) 352–359, https://doi.org/10.17776/csj.1351460.
[19] H.K. Chin, P.Y. Lin, J. Chen, R. Kirankumar, Z.H. Wen, S. Hsieh, Polydopamine-mediated ag and zno as an active and recyclable sers substrate for rhodamine b with significantly improved enhancement factor and efficient photocatalytic degradation, Appl. Sci. 11 (2021), https://doi.org/10.3390/app11114914.
[20] H. Yuan, S. Yu, M. Kim, J.E. Lee, H. Kang, D. Jang, M.S. Ramasamy, D.H. Kim, Dopamine-mediated self-assembled anisotropic Au nanoworms conjugated with MoS2 nanosheets for SERS-based sensing, Sens. Actuat. B Chem. 371 (2022) 132453, https://doi.org/10.1016/j.snb.2022.132453.
[21] P.Y. Lin, G. He, J. Chen, A.K. Dwivedi, S. Hsieh, Monitoring the photoinduced surface catalytic coupling reaction and environmental exhaust fumes with an Ag/PDA/CuO modified 3D glass microfiber platform, J. Ind. Eng. Chem. 82 (2020) 424–432, https://doi.org/10.1016/j.jiec.2019.11.006.
[22] E. Kozma, A. Eckstein Andicsová, A. Opálková Šišková, G. Tullii, F. Galeotti, Biomimetic design of functional plasmonic surfaces based on polydopamine, Appl. Surf. Sci. 591 (2022), https://doi.org/10.1016/j.apsusc.2022.153135.
[23] C. Sun, L. Zhang, R. Zhang, M. Gao, X. Zhang, Facilely synthesized polydopamine encapsulated surface-enhanced Raman scattering (SERS) probes for multiplex tumor associated cell surface antigen detection using SERS imaging, RSC Adv. 5 (2015) 72369–72372, https://doi.org/10.1039/c5ra12628b.
[24] Y. Zhou, J. Zhou, F. Wang, H. Yang, Polydopamine-based functional composite particles for tumor cell targeting and dual-mode cellular imaging, Talanta 181 (2018) 248–257, https://doi.org/10.1016/j.talanta.2018.01.003.
[25] L. Tian, C. Chen, J. Gong, Q. Han, Y. Shi, M. Li, L. Cheng, L. Wang, B. Dong, The convenience of polydopamine in designing SERS biosensors with a sustainable prospect for medical application, Sensors 23 (2023) 1–38, https://doi.org/10.3390/s23104641.
[26] S. Schiavi, A. Taglietti, A. Magni, P. Galinetto, B. Albini, Increasing SERS performance of silver nanoparticles with nanometric coating of polydopamine: a

novel approach for methylene blue detection, Appl. Surf. Sci. 687 (2025) 162223, https://doi.org/10.1016/j.apsusc.2024.162223.
[27] J. Zhou, Q. Xiong, J. Ma, J. Ren, P.B. Messersmith, P. Chen, H. Duan, Polydopamine-enabled approach toward tailored plasmonic nanogapped nanoparticles: from nanogap engineering to multifunctionality, ACS Nano 10 (2016) 11066–11075, https://doi.org/10.1021/acsnano.6b05951.
[28] W.A. Tegegne, M.L. Mekonnen, A.B. Beyene, W.N. Su, B.J. Hwang, Sensitive and reliable detection of deoxynivalenol mycotoxin in pig feed by surface enhanced R1. Tegegne, W.A.; Mekonnen, M.L.; Beyene, A.B.; Su, W.N.; Hwang, B.J. Sensitive and reliable detection of deoxynivalenol mycotoxin in pig feed by surface enhance, Spectrochim. Acta - Part A Mol. Biomol. Spectrosc. 229 (2020). Doi: 10.1016/j.saa.2019.117940.
[29] P. Visciano, M. Schirone, A. Paparella, An overview of histamine and other biogenic amines in fish and fish products, Foods 9 (2020), https://doi.org/10.3390/foods9121795.
[30] T. Janči, D. Valinger, J. Gajdoš Kljusurić, L. Mikac, S. Vidaček, M. Ivanda, Determination of histamine in fish by Surface Enhanced Raman Spectroscopy using silver colloid SERS substrates, Food Chem. 224 (2017) 48–54, https://doi.org/10.1016/j.foodchem.2016.12.032.
[31] E.S. Kolosovas-Machuca, A. Cuadrado, H.J. Ojeda-Galván, L.C. Ortiz-Dosal, A. C. Hernández-Arteaga, M.D.C. Rodríguez-Aranda, H.R. Navarro-Contreras, J. Alda, F.J. González, Detection of histamine dihydrochloride at low concentrations using raman spectroscopy enhanced by gold nanostars colloids, Nanomaterials 9 (2019), https://doi.org/10.3390/nano9020211.
[32] S. Zhang, Q. Fan, J. Guo, X. Jiao, X. Kong, Q. Yu, Surface-enhanced Raman spectroscopy tandem with derivatized thin-layer chromatography for ultra-sensitive on-site detection of histamine from fish, Food Control 138 (2022) 108987, https://doi.org/10.1016/j.foodcont.2022.108987.
[33] F. Gao, E. Grant, X. Lu, Determination of histamine in canned tuna by molecularly imprinted polymers-surface enhanced Raman spectroscopy, Anal. Chim. Acta 901 (2015) 68–75, https://doi.org/10.1016/j.aca.2015.10.025.
[34] T. Zhou, M. Fan, R. You, Y. Lu, L. Huang, Y. Xu, S. Feng, Y. Wu, H. Shen, L. Zhu, Fabrication of Fe3O4/Au@ATP@Ag nanorod sandwich structure for sensitive SERS quantitative detection of histamine, Anal. Chim. Acta 1104 (2020) 199–206, https://doi.org/10.1016/j.aca.2020.01.017.
[35] Z. Wu, E. Xu, A. Jiao, Z. Jin, J. Irudayaraj, Bimodal counterpropagating-responsive sensing material for the detection of histamine, RSC Adv. 7 (2017) 44933–44944, https://doi.org/10.1039/c7ra07362c.
[36] I. Alessandri, M. Zucca, M. Ferroni, E. Bontempi, L.E. Depero, Tailoring the pore size and architecture of Ce02/Ti02 core/shell inverse opals by atomic layer deposition, Small 5 (2009) 336–340, https://doi.org/10.1002/smll.200801249.
[37] K. Lee, M. Park, K.G. Malollari, J. Shin, S.M. Winkler, Y. Zheng, J.H. Park, C. P. Grigoropoulos, P.B. Messersmith, Laser-induced graphitization of polydopamine leads to enhanced mechanical performance while preserving multifunctionality, Nat. Commun. 11 (2020) 5–12, https://doi.org/10.1038/s41467-020-18654-8.
[38] I. Badillo-Ramírez, J.M. Saniger, J. Popp, D. Cialla-May, SERS characterization of dopamine and: In situ dopamine polymerization on silver nanoparticles, Phys. Chem. Chem. Phys. 23 (2021) 12158–12170, https://doi.org/10.1039/d1cp00966d.
[39] A. Meng, B. Cheng, H. Tan, J. Fan, C. Su, J. Yu, TiO2/polydopamine S-scheme heterojunction photocatalyst with enhanced CO2-reduction selectivity, Appl. Catal. B Environ. 289 (2021) 120039, https://doi.org/10.1016/j.apcatb.2021.120039.
[40] I. Alessandri, I. Vassalini, M. Bertuzzi, N. Bontempi, M. Memo, A. Gianoncelli, "RaMassays": synergistic enhancement of plasmon-Free Raman scattering and mass spectrometry for multimodal analysis of small molecules, Sci. Rep. 6 (2016) 1–8, https://doi.org/10.1038/srep34521.
[41] S.L. Kitaw, Y. Wondosen Ahmed, D. Thankachan, A. Candra, T.Y. Wu, B.E. Anley, Y.X. Gou, Y.Y. Chen, Y.T. Cheng, Y.S. Birhan, K.J. Chen, H.C. Tsai, Fabrication of polydopamine functionalized AgNF SERS substrate: applications for sensitive detection of nivalenol in food samples and cell biocompatibility, Colloids Surf. A Physicochem. Eng. Asp. 688 (2024) 133398, https://doi.org/10.1016/j.colsurfa.2024.133398.
[42] J. Fu, Q. Xin, X. Wu, Z. Chen, Y. Yan, S. Liu, M. Wang, Q. Xu, Selective adsorption and separation of organic dyes from aqueous solution on polydopamine microspheres, J. Colloid Interface Sci. 461 (2016) 292–304, https://doi.org/10.1016/j.jcis.2015.09.017.
[43] J. Fu, Z. Chen, M. Wang, S. Liu, J. Zhang, J. Zhang, R. Han, Q. Xu, Adsorption of methylene blue by a high-efficiency adsorbent (polydopamine microspheres): Kinetics, isotherm, thermodynamics and mechanism analysis, Chem. Eng. J. 259 (2015) 53–61, https://doi.org/10.1016/j.cej.2014.07.101.
[44] S.M. Latifi, R. Shankar, H.J. Donahue, Polydopamine coating on titanium affects osteoblastic differentiation to a greater degree than does surface roughness, Adv. Mater. Phys. Chem. 10 (2020) 339–349, https://doi.org/10.4236/ampc.2020.1012027.
[45] S. He, P. Zhou, L. Wang, X. Xiong, Y. Zhang, Y. Deng, S. Wei, Antibiotic-decorated titanium with enhanced antibacterial activity through adhesive polydopamine for dental/bone implant, J. R. Soc. Interface 11 (2014), https://doi.org/10.1098/rsif.2014.0169.
[46] X. Liu, Z. Ye, Q. Xiang, Z. Xu, W. Yue, C. Li, Y. Xu, L. Wang, X. Cao, J. Zhang, Boosting electromagnetic enhancement for detection of non-adsorbing analytes on semiconductor SERS substrates, Chem 9 (2023) 1464–1476, https://doi.org/10.1016/j.chempr.2023.01.017.
[47] D. Wei, S. Chen, Q. Liu, Review of fluorescence suppression techniques in Raman spectroscopy, Appl. Spectrosc. Rev. 50 (2015) 387–406, https://doi.org/10.1080/05704928.2014.999936.
[48] M. Kögler, B. Heilala, Time-gated Raman spectroscopy – a, (2020).
[49] I.A. Mudunkotuwa, V.H. Grassian, Histidine adsorption on TiO2 nanoparticles: an integrated spectroscopic, thermodynamic, and molecular-based approach toward understanding nano-bio interactions, Langmuir 30 (2014) 8751–8760, https://doi.org/10.1021/la500722n.
[50] H. Lee, J. Rho, P.B. Messersmith, Facile conjugation of biomolecu les onto surfaces via mussel adhesive protein inspired coatings, Adv. Mater. 21 (2009) 431–434, https://doi.org/10.1002/adma.200801222.
[51] T. Janči, L. Mikac, M. Ivanda, N. Marušić Radovčić, H. Medić, S. Vidaček, Optimization of parameters for histamine detection in fish muscle extracts by surface-enhanced Raman spectroscopy using silver colloid SERS substrates, J. Raman Spectrosc. 48 (2017) 64–72, https://doi.org/10.1002/jrs.4991.
[52] S.J. Hurst, H.C. Fry, D.J. Gosztola, T. Rajh, Utilizing chemical Raman enhancement: a route for metal oxide support-based biodetection, J. Phys. Chem. C 115 (2011) 620–630, https://doi.org/10.1021/jp1096162.
[53] T.T.H. Pham, X.H. Vu, T.T. Trang, N.X. Ca, N.D. Dien, P. Van Hai, N.T. Ha Lien, N. Trong Nghia, T.t., Kim Chi, Enhance Raman scattering for probe methylene blue molecules adsorbed on ZnO microstructures due to charge transfer processes, Opt. Mater. (Amst.) 120 (2021) 111460, https://doi.org/10.1016/j.optmat.2021.111460.
[54] A. Xie, K. Zhang, F. Wu, N. Wang, Y. Wang, M. Wang, Polydopamine nanofilms as visible light-harvesting interfaces for palladium nanocrystal catalyzed coupling reactions, Catal. Sci. Technol. 6 (2016) 1764–1771, https://doi.org/10.1039/c5cy01330e.
[55] F. Guo, J. Chen, J. Zhao, Z. Chen, D. Xia, Z. Zhan, Q. Wang, Z-scheme heterojunction g-C3N4@PDA/BiOBr with biomimetic polydopamine as electron transfer mediators for enhanced visible-light driven degradation of sulfamethoxazole, Chem. Eng. J. 386 (2020) 124014, https://doi.org/10.1016/j.cej.2020.124014.